International Journal of Biological, Life and Agricultural Sciences
ISSN: 2415-6612
Vol:10, No:8, 2016

Green Synthesis of Nanosilver-Loaded Hydrogel Nanocomposites for Antibacterial Application

D. Berdous, H. Ferfera-Harrar

***Abstract*—**Superabsorbent polymers (SAPs) or hydrogels with three-dimensional hydrophilic network structure are high-performance water absorbent and retention materials. The in situ synthesis of metal nanoparticles within polymeric network as antibacterial agents for bio-applications is an approach that takes advantage of the existing free-space into networks, which not only acts as a template for nucleation of nanoparticles, but also provides long term stability and reduces their toxicity by delaying their oxidation and release. In this work, SAP/nanosilver nanocomposites were successfully developed by a unique green process at room temperature, which involves in situ formation of silver nanoparticles (AgNPs) within hydrogels as a template. The aim of this study is to investigate whether these AgNPs-loaded hydrogels are potential candidates for antimicrobial applications. Firstly, the superabsorbents were prepared through radical copolymerization via grafting and crosslinking of acrylamide (AAm) onto chitosan backbone (Cs) using potassium persulfate as initiator and N,N'-methylenebisacrylamide as the crosslinker. Then, they were hydrolyzed to achieve superabsorbents with ampholytic properties and uppermost swelling capacity. Lastly, the AgNPs were biosynthesized and entrapped into hydrogels through a simple, eco-friendly and cost-effective method using aqueous silver nitrate as a silver precursor and curcuma longa tuber-powder extracts as both reducing and stabilizing agent. The formed superabsorbents nanocomposites (Cs-g-PAAm)/AgNPs were characterized by X-ray Diffraction (XRD), UV-visible Spectroscopy, Attenuated Total reflectance Fourier Transform Infrared Spectroscopy (ATR-FTIR), Inductively Coupled Plasma (ICP), and Thermogravimetric Analysis (TGA). Microscopic surface structure analyzed by Transmission Electron Microscopy (TEM) has showed spherical shapes of AgNPs with size in the range of 3-15 nm. The extent of nanosilver loading was decreased by increasing Cs content into network. The silver-loaded hydrogel was thermally more stable than the unloaded dry hydrogel counterpart. The swelling equilibrium degree (Q) and centrifuge retention capacity (CRC) in deionized water were affected by both contents of Cs and the entrapped AgNPs. The nanosilver-embedded hydrogels exhibited antibacterial activity against *Escherichia coli* and *Staphylococcus aureus* bacteria. These comprehensive results suggest that the elaborated AgNPs-loaded nanomaterials could be used to produce valuable wound dressing.

***Keywords*—**Antibacterial activity, nanocomposites, silver nanoparticles, superabsorbent hydrogel.

I. Introduction

HYDROGELS or SAPs are hydrophilic bicomponent systems consisting of three-dimensional networks of polymer chains and liquid that fills the space between macromolecules. Hydrogels have the possibility of absorbing large amounts of water and biological fluids, and therefore, they are often used in biomedical applications such as hygienic and wound dressings [1]-[3].

While considering hydrogels synthesis, its biocompatibility is an important parameter for biomedical applications. Synthesis of biocompatible hydrogel matrix from a nontoxic, economical, and available materials, such as polysaccharides, is more advantageous than that from synthetic polymers. However, a potential problem for this bio-application is that microorganisms may grow in hydrogel materials because of their natural biocompatible properties. So, the incorporation of antibacterial agents is required. Recent studies have shown that AgNPs are effective as antimicrobial agents, both *in vivo* and *in vitro*, as compared to bulk or ions silver forms, due to their enhanced permeation and retention effects [4]. However, their preparation is difficult because they easily agglomerate. Hence, AgNPs-embedded hydrogels, wherein hydrophilic network act as template and protect nanoparticles from aggregating, have attracted great attention [5]-[7]. Hydrogels impart excellent stability to AgNPs and reduce their toxicity by delaying their oxidation and release. The hydrogel/AgNPs dressings are considerably better than fabrics or films for treating skin burns because they provide an efficient physical barrier against external bacteria, thereby maintaining a humid environment around the wound surface, which is very helpful for the cicatrization process. Since the hydrophilic surface of the soft and gummy hydrogels exhibits a very low interfacial free energy in contact with biological fluids, proteins and cells do not tend to adhere to their surface and no irritation to the surrounding tissues will occur [8].

The biosynthesis of nanoparticles using plant extracts, which represents a connection between biotechnology and nanotechnology, has received increasing consideration due to the growing need to develop eco-friendly technologies for material syntheses. In this paper, we report on the synthesis and characterization of AgNPs-loaded polymer superabsorbent nanocomposites chitosan-graft-polyacrylamide (Cs-g-PAAm) using Curcuma longa tuber-powder extracts as environmentally benign and facile approach. Crosslinked polyacrylamide (PAAm) is widely used in the fields of biomedical applications. Similarly, chitosan Cs, a derivative of chitin polysaccharide, was selected for the preparation of nanocomposites. It is gaining increasing attention owing to its outstanding biological properties like biodegradability, biocompatibility and antibacterial activity [9]. Also, it has been chemically modified by grafting and by forming composites for improving its adsorption properties. The

H. Ferfera-Harrar is with the Department of macromolecular chemistry, University of Sciences and Technology Houari Boumediene USTHB, 16111, Algiers, Algeria (e-mail: harrarhafida@ yahoo.fr).

D. Berdous is with the Department of Chemistry and physics of inorganic materials, University of Sciences and Technology Houari Boumediene USTHB, 16111, Algiers, Algeria (e-mail: berdousiness@yahoo.fr).

reactive NH_2 and OH groups of Cs are convenient for grafting-copolymerization of hydrophilic monomers like acrylamide [10], which could not only enhance hydrophilicity of the Cs backbone and improve biodegradability of chitosan-based superabsorbent materials, but also reduce dependence on petrochemical-derived.

The aim of study was to investigate whether these hydrogels have the potential to be used in bio-applications.

II. Experimental Section

A. Materials

Chitosan (Cs) with 75% deacetylated, medium molecular weight, and viscosity 200-800 cps was purchased from Aldrich. Acrylamide (AAm), Potassium persulfate (KPS) and N,N'-methylene bisacrylamide (MBA), silver nitrate ($AgNO_3$) from Fluka and all other chemicals products of analytical grade were used as received without further purification. The Curcuma longa tubers were purchased from a local market. The bacteria used for antibacterial tests are gram positive *Staphylococcus aureus* (ATCC 6538), and gram negative *Escherichia coli* (ATCC 8739). Doubly distilled water was used for synthesis and swelling studies.

B. Preparation of Curcuma Extract

The C. longa tubers were washed to remove the adhering possible impurities and dried under sunlight for two days to remove moisture. Then the tubers were powdered in a mixer, and then sieved to get uniform size range. Then, 20 g of C. longa tuber powder was added to 400 mL double distilled water and heated for 5 min. and filtered through PVDF Millex Filter. The CC extracted solutions were stored at 4 °C.

C. Synthesis of AgNPs-Loaded Hydrogel Nanocomposites

The hydrogels with different Cs contents were prepared via graft-copolymerization of AAm monomer onto Cs backbone and crosslinking in aqueous solution at 60 °C, according to the standard procedure described in our earlier study [10]. Briefly, an appropriate amount of Cs was dissolved in 30 mL 1% (v/v) acetic acid solution in three-neck flask, equipped with reflux condenser, nitrogen line. After being purged with nitrogen, the flask was placed in bath at 60 °C for 30 min. Then, KPS was added and the resulting mixture was gently stirred for an additional 15 min to generate radicals. Following this, the mixed solution of AAm and MBA, previously purged with inert gas, was added to the flask. The resulting hydrogel was neutralized to pH 8, washed repeatedly in distilled water, dehydrated in excess of methanol and dried in an oven. The obtained grafted Cs-g-PAAm was hydrolyzed at 95 °C for 2 h in alkaline solution, neutralized by acid solution, dewatered with methanol and then dried in oven at 60 °C. Finally, each product was ground at particles size about 40-60 mesh and stored away from moisture, heat and light.

During the hydrolysis treatment, the ammonia evolves and carboxamide groups of PAAm are converted to carboxylate ions (COO^-). Therefore, the structure of the hydrolyzed Cs-g-PAAm hydrogel is composed of amide $COONH_2$ and amine NH_2 groups as well as carboxylate COO^-ions, resulting in hydrogels with ampholytic properties. The mechanism of the formation of hydrolyzed grafted network is illustrated in Fig. 1.

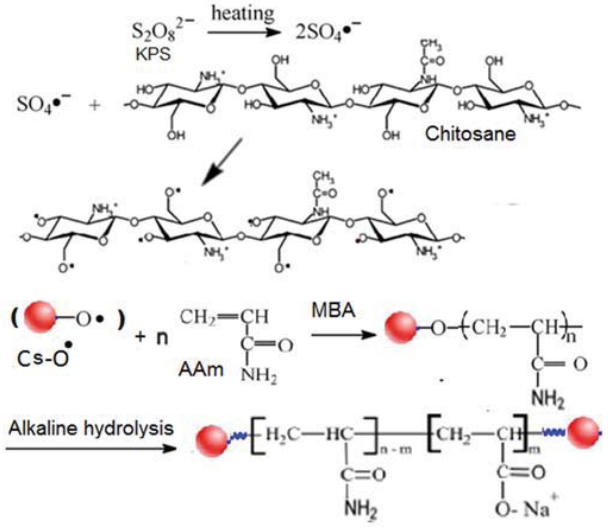

Fig. 1 Mechanistic pathway for the synthesis of the hydrolyzed grafted Cs-g-PAAm hydrogel

Nanosilver particles-loaded hydrogel nanocomposites were prepared by green method based on the reduction of silver ions to metallic AgNPs using curcuma longa extract as reducing agent. Dry hydrogel samples (1g) were equilibrated in 100 ml of distilled water, and then 50 ml of $AgNO_3$solution (2 mM or 0.2 mM) was added and allowed for 24 h. During this equilibrium stage, the Ag^+ ions are being exchanged from solution to the hydrogel networks. The Ag^+ ions loaded Cs-g-PAAm hydrogels were transferred to a beaker containing 60 ml of curcuma in order to reduce the Ag^+ ions into AgNPs. Description of nanocomposites synthesis is given in Fig. 2.

D. Characterizations

XRD analysis was performed on Bruker D8 Advance diffractometer (CuKα radiation, λ = 0.1541 nm) to identify the formed AgNPs. UV–Vis absorption spectra of hydrogel/ AgNPs nanocomposites were recorded on UV–visible spectrophotometer model JASCO V-650 with a scan range of 200–800 nm. ATR-FTIR spectra were performed on Bio-Rad spectrometer model FTS-162. Detection of silver conversion in the gels was quantified by elemental analysis using ICP Prodigy, LEEMAN. The dried sample was treated by 0.3N nitric acid solutions for 1day to induce the oxidation of all of the AgNPs into Ag^+ ions. The morphology of the hydrogels was observed with Scanning Electron Microscope (SEM) HITACHI S-4800 operating at 15 kV. TEM images were recorded using a JEOL, JEM 100CX operating at 80 kV. It was used to find out the size of AgNPs inside hydrogel nanocomposites. TEM sample was prepared by dropping finely grinded nanocomposite dispersion (1 mg/1 ml) on a copper grid and dried at ambient temperature under heating lamp. The AgNPs sizes were measured using Image J

software. Thermal stabilities were studied using TGA analysis on a Q500 analyzer, TA instruments, at 10 ºC/min and under nitrogen atmosphere.

E. Swelling Measurements by Tea Bag Method

The swelling capacities of AgNPs free- or loaded-hydrogels were investigated in an excess of deionized water.

The tea bag, made of 250 mesh nylon screen, containing the pre-weighted dry sample was immersed in water for one day at room temperature to reach the equilibrium, and then hung up to drain the excess solution for 30 min. All experiments were performed in triplicate. The equilibrium water absorbency (Q) was calculated by (1):

$$Q = \frac{W_{tb} - W_b - W_d}{W_d} \quad (1)$$

where Q is the water absorbency defined as grams of water per gram of the xerogel sample, W_{tb} is the weight of both the tea bag and swollen sample, W_b is the weight of the tea bag, and W_d is the weight of the dried sample.

F. Antibacterial Tests

Antibacterial activity of the Cs-g-PAAm hydrogels and Cs-g-PAAm/AgNPs nanocomposites was assessed against the common pathogenic bacteria *Staphylococcus aureus* (Gram+) and *Eschericha coli* (Gram-) qualitatively using the disc diffusion method by measuring the inhibited growth around the sample. The overnight grown culture of bacteria at 37 °C were diluted to reach a concentration of 10^8 colony forming unit/ml (CFU/ml) and plated on LB agar. Equally weighed samples of swollen unloaded-hydrogels and their AgPNs-loaded hydrogels were kept on the plates and incubated at 37 °C for 24 h. The plates were taken out, and the inhibition zone was observed.

The bacteria counting method was also adopted to evaluate the bactericidal activity of the as-prepared hydrogels and their nanocomposites [11]. In this case, the samples were placed in contact with bacteria liquid suspension and subjected to gentile 160 rmp shaking at 37 °C. At zero and 24 h contact times, 100 µL of each suspension were collected and the bacterial number (CFU) was counted by plating in Petri containing LB agar. The same procedure was performed on stain as control.

III. Results and Discussion

A. Evidence for the Formation of Nanocomposite Hydrogel

The procedure for the Cs-g-PAAm/AgNPs nanocomposite synthesis consists of three steps, as illustrated in Fig. 2: (i) the preparation of P Cs-g-PAAm hydrogels; (ii) the loading of Ag+ ions via swelling method; and, (iii) the biosynthesis of AgPNs within Cs-g-PAAm network via green process using Curcuma longa extract. The reduction of Ag^+ into AgNPs during exposure to water extract of *C. longa* tuber powder was able to be followed by the color change. Thus, the formation of AgNPs is evidenced by the change from colorless (neat hydrogel) to brown shades (nanocomposite hydrogels), which is due to the surface-plasmon resonance (SPR) phenomenon.

The extract of *C. longa*, as an aldehyde, forms with Ag^+ the $[Ag\ (C.\ longa)]^+$ complex, which reacts with aldehyde groups in the molecular structure of the methanolic extract and induces the reduction of silver ions through the oxidation of aldehyde to carboxylic acid groups [Ag (*C. longa*)] [12].

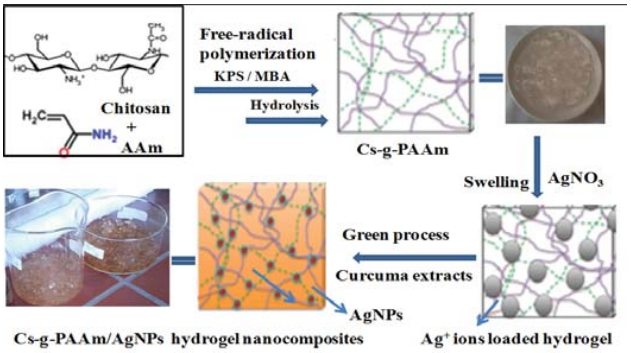

Fig. 2 Schematic synthesis of the Cs-g-PAAm/AgNPs hydrogel nanocomposites

The successful preparation of AgPNs-loaded hydrogel nanocomposite is evidenced by UV–vis absorption studies, Fig. 3. Usually, silver (Ag) nanoparticles exhibit unique and tunable optical properties due to their surface plasmon resonance (SPR) that is dependent on shape, size and size distribution of the nanoparticles [13].

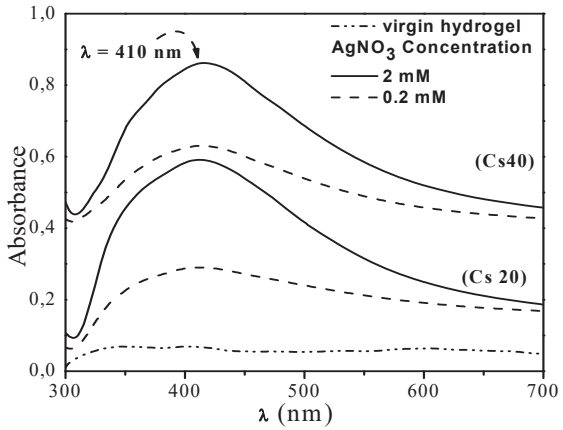

Fig. 3 UV–vis spectra of Cs-g-PAAm hydrogels and its AgNPs-loaded nanocomposite

As can be seen from Fig. 3, the hydrogel nanocomposites spectra show the characteristic plasmonic resonance peak of AgNPs with center of symmetry (spherical or cubic particles) at around 410 nm, while no intense peaks are observed in free hydrogels. Also, the intensity changes of the peaks indicate that the content of AgNPs in the network increase by decreasing the Cs content and increasing the $AgNO_3$ solution concentration in the hydrogel.

The determination of AgNPs within the hydrogels templates, prepared at different amounts of Cs and Ag^+, were

evaluated by elemental analysis using ICP analysis and the results are collected in Table I. The influence the Cs content in the Cs-g-PAAm template on the AgNPs formation is clearly observed. Indeed, the grafted network that contains the highest Cs chains displays a denser microstructure, which might retard the Ag^+ penetration into the inner zone of the network, and thus producing a lower AgNPs content. In this case, the AgNPs loading may close to surface, and so induce a higher size of the AgNPs. Also, there is more probability aggregation of silver particles, resulting in larger clusters of nanoparticles.

TABLE I
DESCRIPTION OF AGNPS-LOADED NANOCOMPOSITES

Cs (wt.%) in Hydrogel	AgNPs content (wt. %) from AgNO3 solution	
	0.2 mM	2 mM
Cs 20	1.3254	2.7714
Cs 40	0.3152	0.7146

At the next stage, the crystalline structure of AgNPs was estimated by XRD. The obtained patterns of hydrogel/silver nanocomposites are presented in Fig. 4. The peaks at 2 θ = 38.5°, 44.4°, 64.5°, and 76.8° are assigned to the crystal planes (111), (200), (220), and (311), respectively, of silver Ag^0 with a face-centered cubic crystal structure [13]. The strong and sharp peak at 2θ =38° suggests the formation of highly crystalline AgNPs. However, virgin hydrogels did not show any such peaks. Thus, it is concluded that hydrogel nanocomposites contain AgNPs.

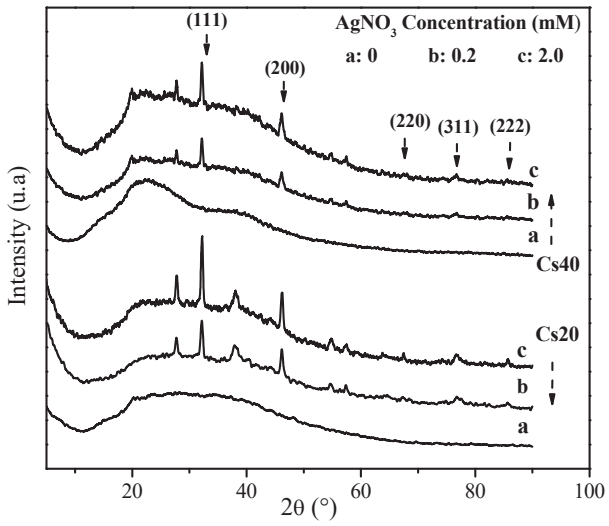

Fig. 4 XRD patterns of Cs-g-PAAm hydrogels and its AgNPs-loaded nanocomposite

The crystalline domain size (CD) of the AgNPs can be estimate by XRD measurement using the Scherrer diffraction formula (2):

$$\frac{k\lambda}{\beta \cos\theta} \quad (2)$$

where k= 0.9 is a kinetic Scherrer constant for the cubic structure, λ= 1.541 Å, β is the peak angular width at half-height, and θ is the diffraction angle. From the Scherrer equation, the crystalline average sizes of AgNPs for all the samples are found to be lower than 15 nm.

The FTIR-ATR spectral comparison of free- and loaded-AgNPs hydrogels, which were prepared from 2 mM $AgNO_3$, is shown from spectra in Fig. 5. It is obvious that all characteristic bands are attributable to the functional groups of grafted network Cs-g-PAAm. These include mainly: the broad band centered at 3290 cm^{-1} due to stretching vibrations of NH (ν_{N-H}) from amide and amine groups as well as OH groups (ν_{O-H}, symmetric). The band at 1664 cm^{-1} ascribes to stretching vibrations of carbonyl ($\nu_{C=O}$) from acetyl and amide groups, and the bands at 1552 and 1404 cm^{-1} are due to stretching vibrations), asymmetric and symmetric respectively, of carbonyl ($\nu_{C=O}$ from carboxylate anions. The bands at 1450 and 1324 cm^{-1} are ascribed to deformation vibrations of C-N (δ_{CO-NH}) and hydroxyl (δ_{O-H}), respectively [14]. In addition, the bands of carbonyl $\nu_{C=O}$ at 1664 cm^{-1} and 1404 cm^{-1} in free-nanosilver hydrogels shifts slightly to lower wavenumbers by 15 and 8 cm^{-1}, respectively, in hydrogel nanocomposite spectra. As a result, it can be concluded that nanosilver nanoparticles are entrapped within hydrogel and that their stabilization occurs over interactions such as chelation between some carboxylate ions groups of the hydrogel networks and AgPNs.

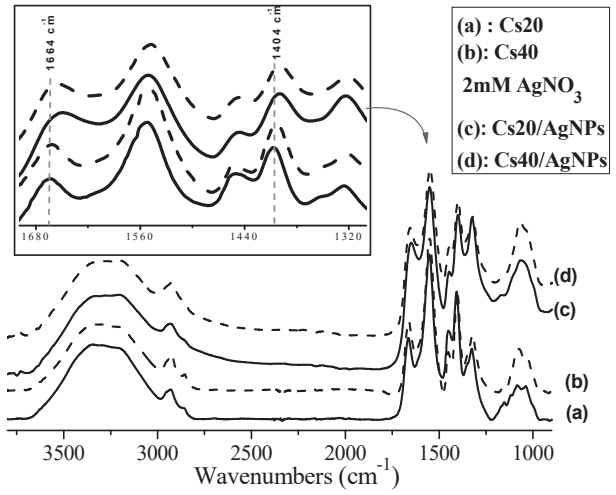

Fig. 5 FTIR-ATR spectra of Cs-g-PAAm hydrogels and its nanocomposites prepared with 2mM of $AgNO_3$

The TEM imaging was also employed to further confirm the formation of AgNPs and to determine their size and morphology. Fig. 6 represents a micrograph of a typical hydrogel sample with upper wt.% AgNPs loading.

The AgNPs have spherical shape and narrow particle size distributions with diameters in the range of 3.66-15 nm, which is also in line with the XRD results. Moreover, the average size and standard deviation is ~ 8 ± 2 nm.

It is evident that Ag^0 nanoparticles are highly stabilized

using the grafted hydrogel template since a few of them are aggregated; confirming that some specifics interactions took place between Ag^0 nanoparticles and both compounds of the Cs-g-PAAm hydrogels.

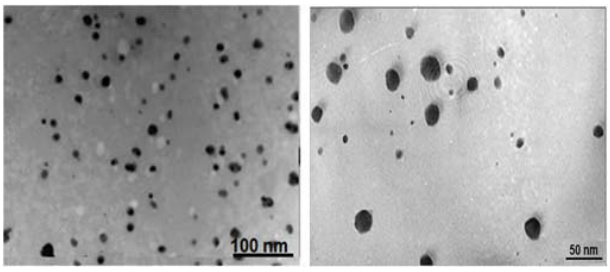

Fig. 6 TEM micrograph of typical Cs-g-PAAm/AgNPs hydrogel nanocomposite ($AgNO_3$= 2 mM, Cs content 20 wt.%)

B. Swelling Properties

As is well known, a porous structure is important for the transport of oxygen and promotion of drainage during wound healing, and a three-dimensional network structure is crucial to absorbing and keeping large amount of water in super-absorbing materials. Also, the surface porosity has great importance on swelling behavior of hydrogels.

The SEM micrographs of the grafted Cs-g-PAAm, observed in Fig. 7, show a porous structure with smooth surface morphology. For the hydrogel samples, the pore diameter distributions were between 200 mm and 500 mm, which were expected to be convenient for the permeation of water, nutrients, oxygen and waste products from the cells. These pores are the sites for interaction of external stimuli with the hydrophilic groups of the network.

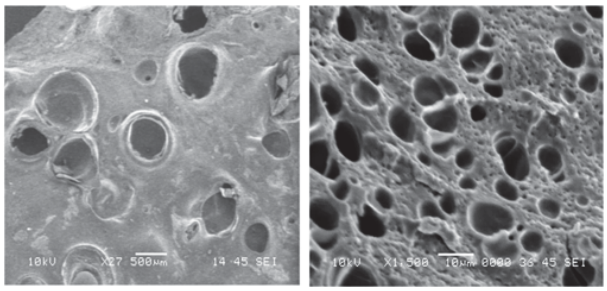

Fig. 7 SEM micrographs of crosslinked Cs-g-PAAm

The swelling properties of hydrogels mainly depend on the hydrophilic ability of the functional groups and the effective crosslink density of the hydrogels. The absorption equilibrium occurred when the values of the osmotic force driving the solvent into the network and the elastic force of the stretched sub-chains became equal.

Fig. 8 shows the swelling behavior as equilibrium degree Q and CRC of free-AgNPs hydrogels and the nanosilver-loaded hydrogel nanocomposites counterparts in deionized water. In an aqueous medium the carboxylate groups were ionized and the electrostatic repulsions between $-COO^-$ groups cause an enhancement in swelling capacity. As the Cs content increases the water absorbing ability is reduced. As previously reported [14], the Cs can act as a multifunctional crosslinker throughout both covalent and hydrogen bonding between its functional groups and those of PAAm to form more junctions in the network that increase the effective crosslinking density, and thus reduce swelling. Likewise, the amount of initiator APS is set and the radical active sites on Cs chains generated by the initiator decomposition is also invariable in the polymerization feed. So, as the Cs content increases, the viscosity of the medium increases gradually that would delay the diffusion of monomers to active sites to produce crosslinked hydrogels, and thus reduces graft efficiency and water absorbency. Consequently, hydrogel containing 20 wt. % of Cs shows the highest equilibrium and CRC values.

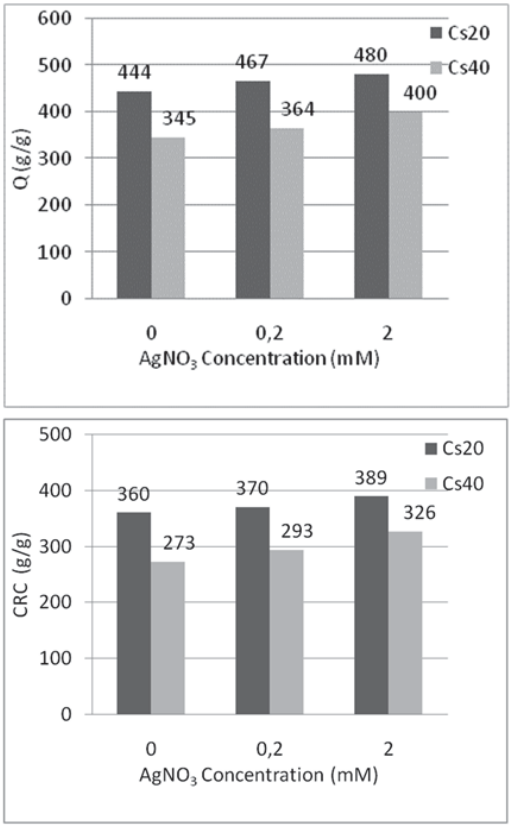

Fig. 8 Swelling properties of Cs-g-PAAm hydrogels and its silver-loaded nanocomposites in distilled water

Overall, each nanosilver-loaded hydrogel Cs-g-PAAm exhibits a slight increase in swelling capacity compared to the unloaded hydrogel counterpart. Similar behavior has been reported in numerous hydrogel/nonosilver studies [15]-[17]. The maximal degree of swelling was raised by increasing the concentrations of $AgNO_3$ precursor solutions, implying that AgNPs would reduce the crosslinking density. This greater absorption rate of nanocomposites is probably caused by the presence of some amounts of dissolved Ag^+ ions that can generate an osmotic gradient. Another reason being that when Ag^+ ions-loaded hydrogels were treated with C. longa extract,

with the addition of many Ag^+ ions, it led to the formation of the nanoparticles within the hydrogel, expanded the gel networks and promoted higher water molecules uptake capacity. This property is important in the biomedical application of nanocomposite hydrogels for wound dressing applications because, compared to a pure hydrogel, hydrogel/AgPNs can further absorb slight to moderate amounts of wound exudates by swelling that helps in rapid healing of certain wounds. Nevertheless, this result also indicates that the water absorbencies for the free hydrogels are not apparently affected when small amount of AgNPs, less than 2.7 wt. % of AgNPs loading, are incorporated within the network.

C. Thermal Properties

Thermal stability of the hydrogel nanocomposites was also investigated by TGA analysis, since it plays an important role during preparation, storage and recycling of biomaterials.

Fig. 9 illustrates the thermograms of silver-loaded and unloaded dry hydrogel samples. All the samples display two thermal degradation steps. The first step appears from 220 °C to 298 °C is due to both weight losses of NH_2 of amide groups in ammonia form and the crosslinker. The third one, which started at 298 °C and extended to 500 °C, is due to the entire degradation of the chain scission both in PAA and chitosan. This means that these Cs-g-PAAm/AgPNs hydrogel nanocomposites can be subjected to sterilization, which is of primary importance for medical applications.

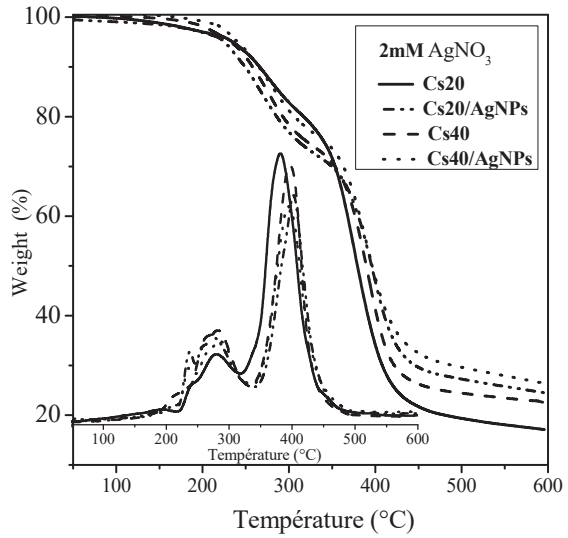

Fig. 9 TGA and dTGthermograms of grafted Cs-g-PAAm hydrogels and its Cs-g-PAAm/AgNPs nanocomposites

Besides, the weight losses up to 580 °C observed for free hydrogels Cs-g-PAAm containing 20 wt. % and 40 wt. % of Cs are 82.61% and 77.46%, respectively, whereas, the counterpart nanocomposites formed after the biosynthesis of nanosilver particles using 2 mM of $AgNO_3$ precursor show only 76.57% and 73.65% at the same temperature. The decrease in the thermal decomposition rate of the AgNPs-loaded hydrogel can be attributed to two reasons. AgNPs have higher thermal stability as compared to the polymeric chains of the hydrogel, and hence, the presences of AgNPs particles induce more stability to the network. The AgNPs may interact with the network through carbonyl and OH groups of PAAm and Cs chains, as indicated by the results of the FTIR study. Such interactions can lead to the formation of some weak intermolecular crosslinks between the polymeric chains that restrict their mobility. Consequently, the degradation process will be slowed down in the presence of AgNPs. In addition, the presence of nanosilver does not catalyze any radical-initiated thermal decomposition reactions, called "nano-effect" [18], of the polymer network that is an important feature for biomedical purposes.

D. In vitro Antibacterial Properties

For checking the antibacterial activity, equally weighed hydrogel and their nanocomposites, were tested against two different bacterial strains; *S. aureus* as an example of Gram positive bacteria and *E. coli* as an example of Gram negative bacteria. The unloaded and loaded hydrogels were subjected to quantitative disc diffusion method, Fig. 10.

After 24 h incubation at 37 °C, the observed inhibitory zones are narrow diameters for the specimens. So, the unloaded hydrogels are found to be just active by contact. This moderate antibacterial activity observed is obviously originated from Cs compound owing to its polycationic structure. Indeed, in diluted acidic medium the positively charged chitosan-NH_3^+ can bind to anionic groups on the cell surface and form polyelectrolyte complexes with the bacterial surface. This disrupts the normal functions of the membrane, e.g. by suppressing its biosynthesis, and thereby promotes the leakage of intracellular components. Besides, the moderate antibacterial activity of these hydrogels can be ascribed to the fact that the tested samples are in a solid form and thus only bacteria in direct contact with active sites of the hydrogels could be inhibited. Indeed, the Cs-based materials have more effective antibacterial ability in dissolved state than in solid one such as in membranes, films and hydrogels systems [19]. Thus, this study aims to improve the antibacterial performance properties of grafted Cs-g-PAAm hydrogel via in situ biosynthesis of bioactive nanosilver particles.

The swollen hydrogel/AgNPs nanocomposites exhibit obvious inhibition zones. Therefore, it can be concluded that the antibacterial activity was mainly ascribed to AgNPs, but not only to the network that serves as a stable carrier for nanosilver particles.

The dynamic shake flask method followed by bacterial counting on plate count agar was conducted to evaluate the antibacterial activity quantitatively. The incubation was performed at 37 °C and oscillated at a frequency of 160 rpm for 24 h. Pure bacteria medium (10^8 CFU/ml) was also incubated and served as control. The bactericidal activity bacterial reduction in %(R) were calculated using (3) and (4):

$$\text{Bactericidal activity} = \log (CFU_{Cont})_0 - \log (CFU_{Hyd})_{24} \quad (3)$$

$$R\ (\%) = \frac{(CFU_{Cont})_{24} - (CFU_{Hyd})_{24}}{CFU_{Cont})_{24}} \times 100 \quad (4)$$

where $(CFU_{Cont})_0$ and $(CFU_{Cont})_{24}$ refers the viable bacterial number for the control sample at 0 and 24 h contact time, respectively, while $(CFU_{Hyd})_{24}$ represent the bacterial survival number for the free hydrogels and the nanocomposites counterparts at 24 h contact time.

The data associated to the detection of the antibacterial efficacy, reported in Table II, reveals that:

(1) All the nanocomposites samples performed exhibit outstanding antibacterial activities owing to the presence of AgNPs compared to free-hydrogel counterparts.
(2) The higher $AgNO_3$ precursor concentration, the higher silver content in network and hence, the better the imparted antibacterial activity.
(3) Regardless of AgNPs loading and Cs content in the hydrogel nanocomposites, the reduction of bacterial colonies was always higher than 85%.

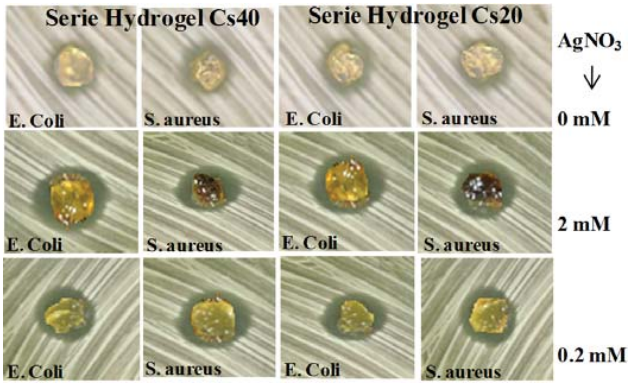

Fig. 10 Antibacterial activity picture of grafted Cs-g-PAAm hydrogels and its Cs-g-PAAm/AgNPs nanocomposites against *S. aureus* and *E. coli* bacteria

It is known that antibacterial activity is considered to be low when the value is less than a 1-log reduction, moderate if the value is between a 1- and 3-log reduction and high for a value greater than a 3-log reduction [20]. Hence, it could be deemed that the nanocomposites exhibited a high antibacterial effect, with the log reduction above three and maximal bacterial reduction about 99.99%. Additionally, it appears that silver nanocomposite hydrogel shows better activity towards *S. aureus* bacteria than *E. coli* and the biocidal activity increases with increase of concentration. Indeed, the structure of the cell wall of *E. coli* (Gram-negative strain) has another outside the peptidoglycan layer that is mainly constructed from tightly packed lipopolysaccharide molecules, resulting in the effective resistive barrier against foreign compounds attack [21]. Besides, disregarding the exact mechanism of the antibacterial activity of AgNPs, several works on AgNPs-based materials have stated that the AgNPs and/or the released silver ions Ag^+, which originate from the partial oxidation of nanosilver particles may increase the cell membrane permeability and, subsequently, penetrate inside cells to interact with the peptidoglycan wall cells and the plasmatic membrane causing direct membranes cell lyses. [22]

Although it is not yet possible to confirm a single mechanism for the antibacterial action of silver, multifaceted antibacterial activity seems to be the key to low bacterial resistance rates observed.

TABLE II
ANTIBACTERIAL PROPERTIES DATA OF FREE- HYDROGELS AND AGNPS-LOADED NANOCOMPOSITES

Cs (wt.%)	AgNPs (wt.%)	CFU /ml *S. aureus/E. coli*	Bactericidal activity (log reduction) *S. aureus/E. coli*	Reduction (%) *S. aureus/E. coli*
Control (Strain)	0	3.52×10^9 / 4.03×10^9	- -	- -
Cs 20	0	1.26×10^9 / 1.50×10^9/	- -	64.204/ 62.786
	1.325	3.50×10^4 / 4.07×10^4	3.456 / 3.390	99.999/ 99.998
	2.771	4.27×10^3 / 4.67×10^3	4.369/ 4.330	99.999/ 99.998
Cs 40	0	1.04×10^9/ 1.27×10^9	- -	70.454 68.486
	0.315	5.40×10^8 / 6.02×10^8	- -	84.659/ 85.062
	0.714	1.00×10^5/ 1.20×10^5	3.000/ 2.930	99.997/ 99.996

IV. CONCLUSION

An effective green process for the fabrication of novel hydrogel/nanosilver nanocomposites via in situ biosynthesize of AgNPs within hydrogel as a template has been described. The formation AgPNs, with a face-centered cubic crystal structure, inside the hydrogels was evidenced by DRX, UV-visible, and ICP analyses. Specifics interactions between t hydrogel and nanoparticles were assessed by FTIR study.

TEM micrographs have showed spherical shape of AgNPs with size less 15 nm.

The effects of the template composition and the concentration of $AgNO_3$ precursor on the AgNPs formation, as well as their loading, were also investigated. TG analysis has revealed that the silver-loaded hydrogel network to be thermally more stable than the un-loaded one. The swelling studies, both the equilibrium absorption and CRC of the hydrogels, having porous structure as observed from SEM image, have been improved by increasing the entrapped Ag^0nanoparticles.The antibacterial studies on the nanosilver-loaded-hydrogels showed good antibacterial activity against the Gram-positive *S. aureus* and Gram-negative *E. coli* bacteria. The quantitative assay by counting method has revealed a high antibacterial effect, with higher reduction ratio above 99.99% after contact with bacteria for 24 h.

Application of these hydrogel/nanosilver nanocomposites based on these findings is expected to lead to valuable discoveries in biomaterials, such as wound dressing materials.

REFERENCES

[1] M.J. Zohuriaan-Mehr, K. Kabiri, "Superabsorbent polymer materials", *Iran. Polym. J.*, vol. 17, pp. 451-477, 2008.
[2] H. Ferfera-Harrar, N. Aiouaz, N. Dairi, "Synthesis and Properties of Chitosan-Graft-Polyacrylamide/Gelatin Superabsorbent Composites for Wastewater Purification", *World Academy of Science, Engineering and*

Technology Inter. J. Chem., Molecular Nuclear Mater. Metallurgical Eng., vol.9, pp.757–764, 2015.
[3] C.Y. Chang, B. Duan, J. Cai, L.N. Zhang, "Superabsorbent hydrogels based on cellulose for smart swelling and controllable delivery", *Eur. Polym. J.*, vol. 46, pp. 92-100, 2010.
[4] M. Rai, A. Yadav, A. Gade, "Silver nanoparticles as a new generation of antimicrobials", *Biotech. Advances*, vol 27, pp.76–83, 2009.
[5] Y. Murali Mohan, K. Vimala, V. Thomas, K. Varaprasad, B. Sreedhar, S.K. Bajpai, K. Mohana Raju, "Controlling of silver nanoparticles structure by hydrogel networks", *J. Colloid Interf. Sci.,* vol. 342, pp. 73–82, 2010.
[6] B. Boonkaew, P. Suwanpreuksa, L. Cuttle, P. M. Barber, P. Supaphol, "Hydrogels Containing Silver Nanoparticles for Burn Wounds Show
[7] Antimicrobial Activity without Cytotoxicity", *J. Appl. Polym. Sci*., vol.131, pp.40215-40225, 2014.
[8] H. Bożena Tyliszczak, K. Pielichowski, "Novel hydrogels containing nanosilver for biomedical applications - synthesis and characterization", *J. Polym. Res*., vol. 20, pp. 191-196, 2013.
[9] K. Varaprasad, Y. Murali Mohan, K. Vimala, K. Mohana Raju, "Synthesis and characterization of hydrogel–silver nanoparticle–curcumin composites for wound dressing and antibacterial application", *J. Applied Polym. Sci*., vol. 121, pp.784–796, 2011.
[10] H. Mellegard, S.P. Strand, B.E. Christensen, P.E. Granum, S.P. Hardy, "Antibacterial activity of chemically defined chitosans: Influence of molecular weight, degree of acetylation and test organism", *Int. J. Food Microbiol.*, vol. 148, pp.48-54, 2011.
[11] H. Ferfera-Harrar, N. Aiouaz, N. Dairi, A. S. Hadj-Hamou, "Preparation of chitosan-g-poly(acrylamide)/montmorillonite superabsorbent polymer composites: Studies on swelling, thermal, and antibacterial properties", *J. Appl. Polym. Sci*., vol.131, pp. 39747-39750, 2014.
[12] K. Vimala, Y.M. Mohan, K. Varaprasad, N. Reddy, S. Narayana Ravindra, N. S. Naidu, "Fabrication of curcumin encapsulated chitosan–PVA silver nanocomposite films for improved antimicrobial activity", *J. Biomaterials and Nanobiotechnology*, vol. 2, pp.55–64, 2011.
[13] K. Shameli Mansor Bin Ahmad, A. Zamanian, P. Sangpour, P. Shabanzadeh, Y. Abdollahi, M. Zargar, "Green biosynthesis of silver nanoparticles using Curcuma longa tuber powder", *Int. J. Nanomedicine*, vol. 7, pp. 5603–5610, 2012.
[14] H. Ferfera-Harrar, N. Aiouaz, N. Dairi, "Environmental-sensitive chitosan-g-polyacrylamide/carboxymethylcellulose superabsorbent composites for wastewater purification I: synthesis and properties", *Polym. Bull*., vol.73, pp.815-840, 2016.
[15] J. Krstic, J. Spasojevic, A. Radosavljevic, A. Peric-Grujic, M. Duric, Z. K. arevic-Popovic, S. Popovic, "*In vitro* Silver Ion Release Kinetics from Nanosilver/Poly(vinyl alcohol) Hydrogels Synthesized by Gamma Irradiation", *J. Appl. Polym. Sci*., vol.131, pp.40321-40335, 2014.
[16] T. Jayaramudu, G. M. Raghavendra, K. Varaprasad, R. Sadiku, K. Ramam, K. Mohana Raju, "Iota-Carrageenan-based biodegradable Ag 0 nanocomposite hydrogels for the inactivation of bacteria", *Carbohyd. Polym*., vol. 95, pp.188–194, 2013.
[17] Y. Zhou, Y. Zhao, L. Wang, L. Xu, M. Zhai, S. Wei, "Radiation synthesis and characterization of nanosilver/gelatin/carboxymethyl chitosan hydrogel", *Radiation Phy. Chem*., vol. 81, pp.553–560, 2012.
[18] S.K. Murthy, Y. Murali Mohan, K. Varaprasad, B. Sreedhar, K. Mohana Raju, "First successful design of semi-IPN hydrogel–silver nanocomposites: A facile approach for antibacterial application", *Colloid. Interf. Sci*., vol. 318, pp.217-224, 2008.
[19] M. Pereda, A.G. Ponce, N.E. Marcovich, R.A. Ruseckaite, J.F. Martucci, "Chitosan-gelatin composites and bi-layer films with potential antimicrobial activity", *Food Hydrocolloid,* vol. 25, pp.1372-1381, 2011.
[20] C. L. Gallant-Behm, H. Q. Yin, S. Liu, J. P. Heggers, R. E. Langford, M. E. Olson, et al., "Comparison of *in vitro* disc diffusion and time kill-kinetic assays for the evaluation of antimicrobial wound dressing efficacy", *Wound Repair and Regeneration*, vol.13, pp. 412–421, 2005.
[21] N. Liu, X.G. Chen, H.J. Park, C.G. Liu, C.S. Liu, X.H. Meng, L.J. Yu, "Effect of MW and concentration of chitosan on antibacterial activity of *Escherichia coli*", Carbohydr. Polym., vol. 64, pp.60-65, 2006.
[22] W. K., Jung, H. C. Koo, K. W. Kim, S. Shin, S. H. Kim, Y. H. Park, "Antibacterial activity and mechanism of action of the silver ion in *Staphylococcus aureus* and *Escherichia coli*". Appl. Environ. Microbiol., vol. 74, pp. 2171-8, 2008.